Characterization of Gaseous Effluents in the LWIR from Both Modeling and Hyperspectral Measurements[1]

Michael K. Griffin[2], John P. Kerekes, Kristine E. Farrar, and Hsiao-hua K. Burke

MIT Lincoln Laboratory, 244 Wood St., Lexington, MA 02420-9185

ABSTRACT

Longwave Infrared (LWIR) radiation comprising atmospheric and surface emissions provides information for a number of applications including atmospheric profiling, surface temperature and emissivity estimation, and cloud depiction and characterization. The LWIR spectrum also contains absorption lines for numerous molecular species which can be utilized in quantifying species amounts. Modeling the absorption and emission from gaseous species using various radiative transfer codes such as MODTRAN-4[1] and FASE[2] (a follow-on to the line-by-line radiative transfer code FASCODE[3]) provides insight into the radiative signature of these elements as viewed from an airborne or space-borne platform and provides a basis for analysis of LWIR hyperspectral measurements.

In this study, a model platform was developed for the investigation of the passive outgoing radiance from a scene containing an effluent plume layer. The effects of various scene and model parameters including ambient and plume temperatures, plume concentration, as well as the surface temperature and emissivity on the outgoing radiance were estimated. A simple formula relating the various components of the outgoing radiance was used to study the scale of the component contributions. A number of examples were given depicting the spectral radiance from plumes composed of single or multiple effluent gases as would be observed by typical airborne sensors. The issue of detectability and spectral identification was also discussed.

1. INTRODUCTION

Detection of effluents from remotely based platforms provides a mechanism to monitor a variety of environmental and geologic conditions over a large region. Volcanic eruptions produce large amounts of SO_2, H_2O and CO_2 which can be detected from high altitude sensors. Oil spills can be monitored by their spectral signature. There is a strong interest in the military to improve our ability to detect and identify biological and chemical releases in the battlespace arena. For example, the Multispectral Thermal Imager (MTI) sensor was designed to aid in the detection of the proliferation of nuclear weapons[4].

[1] This work was sponsored by the Department of Air Force under Contract F19628-00-C-0002. Opinions, interpretations, conclusions and recommendations are those of the authors and not necessarily endorsed by the United States Air Force.

[2] email: griffin@ll.mit.edu; phone 781-981-0396; fax 781-981-7271

Report Documentation Page

Report Date	Report Type	Dates Covered (from... to)
05 Feb 2002	N/A	-

Title and Subtitle Characterization of Gaseous Effluents in the LWIR From Both Modeling and Hyperspectral Measurements	**Contract Number**
	Grant Number
	Program Element Number
Author(s)	**Project Number**
	Task Number
	Work Unit Number
Performing Organization Name(s) and Address(es) MIT Lincoln Laboratory 244 Wood Street Lexington, MA 02420-9185	**Performing Organization Report Number**
Sponsoring/Monitoring Agency Name(s) and Address(es) U.S. Army Aviation and Missle Command ATTN: AMSAM-RD-WS-PL Redstone Arsenal, AL	**Sponsor/Monitor's Acronym(s)**
	Sponsor/Monitor's Report Number(s)

Distribution/Availability Statement
Distribution authorized to U.S. Gov't. agencies and their contractors; (Critical Technology; June 2002). Other requests shall be referred to (AMSAM-RD-WS-PL, Redstone Arsenal, AL 35898-5000).

Supplementary Notes
Proceedings for the Workshop on Multi/Hyperspectral Technology and Applications. See also ADM201485 for entire conference on cd-rom., The original document contains color images.

Abstract

Subject Terms

Report Classification unclassified	**Classification of this page** unclassified
Classification of Abstract unclassified	**Limitation of Abstract** UU

Number of Pages
14

The ability to model hyperspectral scenes which contain effluent emissions from a stack or other source provides the initial foundation for further efforts in effluent detection and remote identification. The simulation of the scene radiance for plume cases was primarily used for development of applications for a hyperspectral system analysis model termed the Forecasting and Analysis of Spectroradiometric System Performance (FASSP[5]). It provides a means for understanding the effects of plumes on the outgoing radiance field and provides a testbed for the ongoing effluent detection and identification study.

In this study, FASE is used to produce estimates of the atmospheric spectral opacity (layered optical depth) from a scene containing an effluent plume layer, which when used in conjunction with a simple radiative transfer algorithm can produce an estimate of the at-sensor radiance. In a previous study, the effects of various scene and model parameters including surface and ambient temperature, plume temperature and concentration and spectral bandwidth on the outgoing radiance were estimated[6]. Results of trade studies on the magnitude of the various parameter contributions to the outgoing radiance showed that plume concentration and temperature were the most significant contributors. In this paper, the relationship between these parameters will be explored in more detail. Using gaseous absorbances from a commercially available spectral library, at-sensor radiances can be modeled for combinations of gases not found in standard line-by-line spectral databases such as HITRAN-96[7]. This provides the opportunity to simulate the measured signal from a controlled release of gases as observed from an airborne or spaceborne sensor. Some examples of these simulations are given in later sections of this paper. Using the FASE line-by-line radiative transfer code, estimates of the at-sensor radiance can be made for a selection of sensor bandwidths, effluent concentrations and temperatures and scene backgrounds. An example of the signal from an atmosphere with a layer of enhanced SO_2 is shown in Fig. 1a. The difficulty in identifying the effluent solely on its radiance is clearly seen. However, if an estimate of the background radiance can be obtained, then the radiance difference due to the enhanced effluent can be estimated. The characteristic double peaked SO_2 absorption signal in the 8.5 μm region is easily recognized in Figure 1b where the spectral range of the plots has been narrowed.

2. RADIATIVE TRANSFER FOR PLUME SCENARIO

To model the at-sensor radiance for a scene containing a plume, some modeling assumptions were made: 1) the enhanced effluent amounts reside wholly within a thin plume layer (nominally 10 m), 2) the temperature is constant over the entire plume layer, and 3) the surface conditions (temperature and emissivity) for the background and underlying the plume are identical. Figure 2 shows a diagram of the various components of the background and plume radiance computation. Ideally, the signature of the effluent can be obtained by subtracting the radiance of a nearby effluent-free location from the radiance through the plume. Radiative transfer equations for both the background and through-plume cases are presented below.

2.1 Clear-sky Radiance

The clear or background radiance can be found by summing the contributions from three components: 1) the path radiance L_{path}, 2) the surface emitted radiance transmitted to the sensor L_{sfc}, and 3) the reflected downwelling radiance transmitted to the sensor L_{refl}. For a single wavelength or narrow-band channel the equation can be written as,

$$L_{bkg} = L_{path} + L_{refl} + L_{sfc} = L_{up} + (1-\varepsilon_{sfc})t_{atm}L_{dn} + \varepsilon_{sfc}B(T_{sfc})t_{atm} \quad (1)$$

where ε_{sfc} and T_{sfc} are the emissivity and temperature of the surface, respectively, B is the Planck function, L_{up} and L_{dn} are the atmospheric upwelling and downwelling radiances,

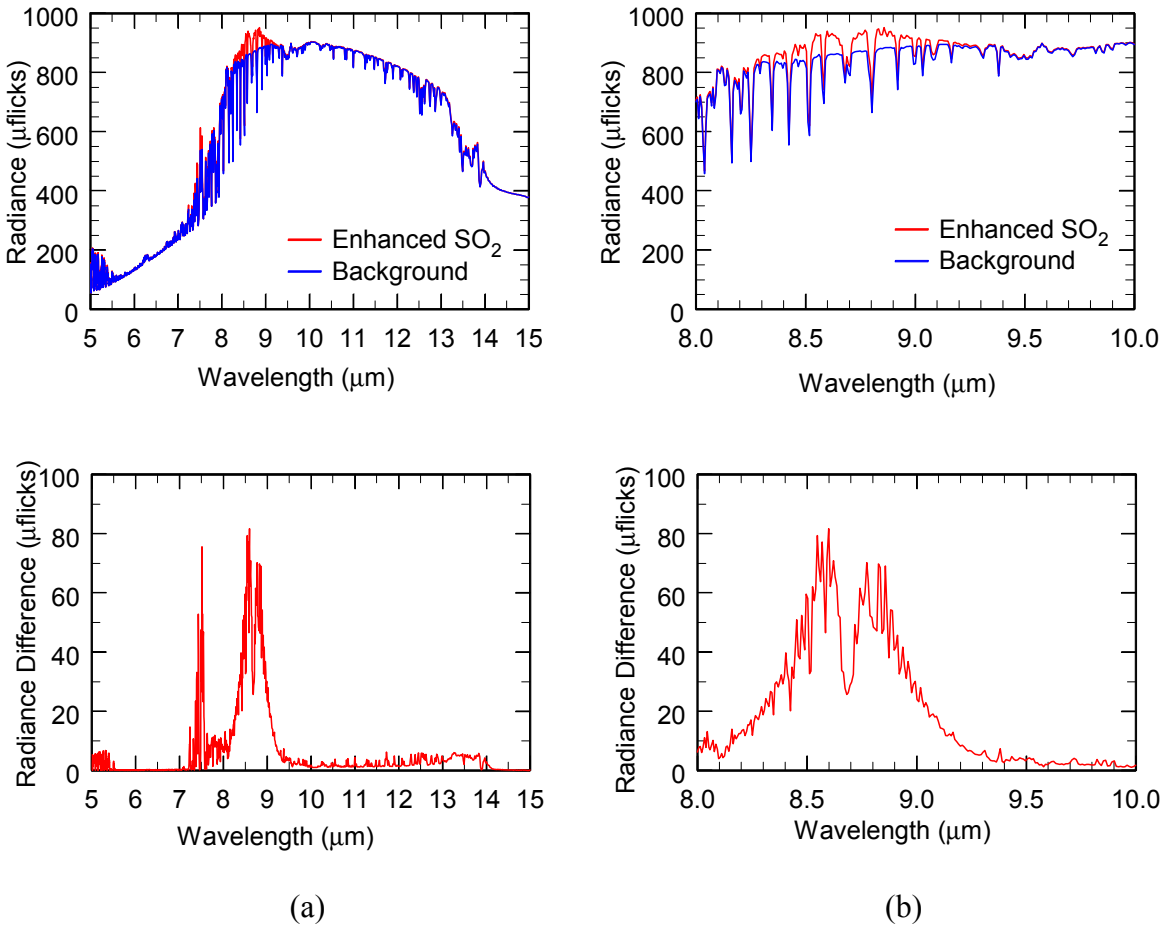

Figure 1. Plots of the radiance in units of μW cm^{-2} sr^{-1} μm^{-1} (μflicks) from a scene with and without an enhanced SO_2 concentration layer. The upper plots provide the simulated radiances at 1 cm^{-1} resolution while the lower plots represent the difference in the two radiance curves. Curves in a) represent the signal across the broad LWIR spectral band while b) narrows the spectral range to that which covers the primary SO_2 absorption band.

respectively, and t_{atm} is the atmospheric transmittance from surface to sensor. Each of the full atmospheric parameters can be separated into individual components arising from below, above and within the plume layer as depicted in Fig. 2. For the background case there is no plume so the plume layer is treated as a thin model layer with appropriate amounts of all gases. Therefore, we can define the atmospheric parameters in (1) by their component values,

$$\begin{aligned} L_{up} &= L_{up}^{a} + (1 - t_{p*}) B[T_{p*}] t_a + L_{up}^{b} t_{p*} t_a \\ L_{dn} &= L_{dn}^{b} + (1 - t_{p*}) B[T_{p*}] t_b + L_{dn}^{a} t_{p*} t_b \\ t_{atm} &= t_b t_{p*} t_a \end{aligned} \quad , \tag{2}$$

where the sub/superscripts *b, a* and *p** on the transmission and radiance represent below, above and in-plume layer values, respectively. The above-plume transmission t_a refers to the path from the top of the plume layer to the sensor. This also applies to the atmospheric transmission t_{atm} and the upwelling radiance $L_{up}{}^{a}$. The downwelling radiance $L_{dn}{}^{a}$ is measured over the entire atmospheric path from top-of-atmosphere to the plume layer. Upon substitution (1) becomes,

$$\begin{aligned} L_{bkg} = {} & L_{up}^{a} + (1 - t_{p*}) B[T_{p*}] t_a + L_{up}^{b} t_{p*} t_a && (path) \\ & + \left\{ \left(L_{dn}^{a} t_{p*} + (1 - t_{p*}) B[T_{p*}] \right) t_b + L_{dn}^{b} \right\} (1 - \varepsilon_{sfc}) t_b t_{p*} t_a && (refl) \\ & + \varepsilon_{sfc} B[T_{sfc}] t_b t_{p*} t_a && (sfc) \end{aligned} \quad . \tag{3}$$

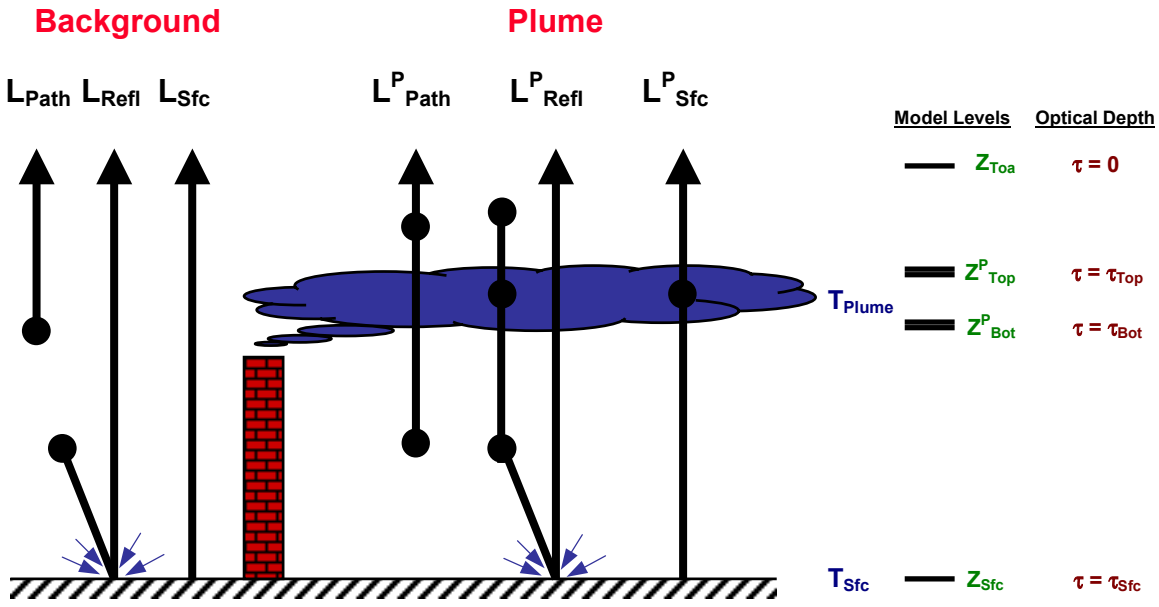

Figure 2. Graphic depicting the contributions from the surface, plume layer and atmosphere to the at-sensor radiance. The model levels are shown as a function of altitude.

It can be shown that some components provide a small or negligible contribution to the overall signal. The plume layer and below plume layer transmissions t_b and t_{p*}, respectively, are very close to 1. The downwelling radiance from below the plume layer L^b_{dn} is much smaller than that from above the plume layer. Likewise for the upwelling radiance L^b_{up}. If these assumptions are followed then (2) reduces to $L_{up} = L^a_{up}$, $L_{dn} = L^a_{dn}$ and $t_{atm} = t_a$ and (1) can be written in the form,

$$L_{bkg} = L_{path} + L_{refl} + L_{sfc} = L^a_{up} + \left(1-\varepsilon_{sfc}\right) t_a L^a_{dn} + \varepsilon_{sfc} B\left[T_{sfc}\right] t_a \ . \tag{4}$$

The atmospheric parameters L^a_{up}, L^a_{dn} and t_a, can be estimated from initial scene conditions using an appropriate radiative transfer model. The surface temperature T_{sfc}, may be known from supplementary data, while the surface emissivity ε_{sfc}, a function of wavelength, must be retrieved.

2.2 Radiance Through a Plume

When a plume layer is added to the scene, the contributions to each of the three components become more complex. While most radiative transfer models do not calculate the individual components associated with the inclusion of a plume (they do not treat the plume layer any differently from one with standard amounts of effluent), it is of interest to determine the scale of the contributions from each of the locations denoted by a solid circle in Fig. 2. The radiance equation for a case with a plume layer has the form,

$$\begin{aligned} L_{plume} &= L^P_{path} + L^P_{refl} + L^P_{sfc} \\ &= L^a_{up} + L^b_{up} t_p t_a && (path) \\ &+ \{(L^a_{dn} t_p + (1-t_p) B[T_p]) t_b + L^b_{dn}\} (1-\varepsilon_{sfc}) t_b t_p t_a && (refl) \\ &+ \{\varepsilon_{sfc} B(T_{sfc}) t_b t_p + (1-t_p) B[T_p]\} t_a && (sfc) \end{aligned} \ , \tag{5}$$

where the sub/superscripts b and a on the transmission and radiance represent below and above-plume layer values, respectively, and where the sub/superscripts p on the transmission and radiance represent the in-plume layer value while $p*$ in (2) above represented the same layer but for a clear scene. In this case the transmission through and radiance emitted from the plume layer can not be neglected. Some terms in (5) have a relatively small impact on the overall at-sensor radiance. Griffin, et al [6] computed the percent contribution for each of the terms in (2) and (5) for a selection of simulated effluent emissions. The dominant term for background (no plume) conditions is the surface emission term which contributes to 93-95 % of the radiance. Emission from the plume is the dominant term as expected in the effluent absorption band. The results showed that reflection terms are mostly negligible because of the low reflectance of the surface (generally less than 0.1 in the LWIR) and the path radiance (excluding the plume contribution) contributes 5-8% of the total radiance.

2.3 Differential Radiance

The radiance difference ΔL between the scene with a plume and the background can be found by subtracting (2) from (5), and assuming the transmission through the "clear" thin plume layer t_{p*} is 1,

$$\Delta L = t_a\left(1-t_p\right)\left\{\begin{array}{l} B\left[T_p\right]\left\{1+t_b^2\left(1-\varepsilon_{sfc}\right)t_p\right\} \\ \quad -\left\{L_{up}^b + L_{dn}^b\left(1-\varepsilon_{sfc}\right)t_b + \varepsilon_{sfc}B\left[T_{sfc}\right]t_b\right\} \\ \quad -\left(1+t_p\right)L_{dn}^a t_b^2\left(1-\varepsilon_{sfc}\right) \end{array}\right\} . \tag{6}$$

To simplify the equation, we will apply the assumptions made above for the upwelling and downwelling radiance below the plume ($L^b_{up} << L^a_{up}$; $L^b_{dn} << L^a_{dn}$) and for the transmittance for that layer ($t_b \sim 1$) to (6), which now reduces to,

$$\Delta L = t_a\left(1-t_p\right)\left\{B\left[T_p\right] - \varepsilon_{sfc}B\left[T_{sfc}\right] + \left(1-\varepsilon_{sfc}\right)\left\{B\left[T_p\right]t_p - \left(1+t_p\right)L_{dn}^a\right\}\right\} . \tag{7}$$

The third component within the parenthesis is a form of the reflected downwelling radiance. From Griffin, et al [6], the contribution from the reflected downwelling radiance accounts for less than 3 % of the total radiance differential value depending on the plume temperature and transmission and the surface emissivity. Neglecting the downwelling radiance term simplifies (7) considerably and is done here. The equation reduces to the approximate form,

$$\Delta L \cong t_a\left(1-t_p\right)\left\{B\left[T_p\right] - \varepsilon_{sfc}B\left[T_{sfc}\right]\right\} , \tag{8}$$

which illustrates the three factors that appear to have the most effect on the detection of an effluent: 1) the atmospheric transmission from the plume to the sensor, 2) the emissivity of the plume, and 3) the relative radiance difference between the plume and the surface. The first factor, the atmospheric transmission influences the effluent signature by attenuating the overall signal. It affects both the background and plume emissions equally (assuming the atmosphere conditions are unchanging over the scene). The second factor, the emissivity of the plume is a function of the transmission of the plume layer and therefore is directly related to the concentration of effluent in the plume layer. Lower plume layer transmission (a result of increased effluent amount), acts to increase ΔL. Conversely, the plume emissivity tends toward zero (as does ΔL) when the effluent concentration is small. The third factor which relates the plume layer radiance and the surface emitted radiance is a function of the plume and surface temperature and the surface emissivity. Here the contrast in the plume versus surface temperature affects not only the magnitude of the signal but the direction of the signal as well. If the surface temperature is significantly greater than the plume temperature (i.e., hot sand, pavement or concrete), ΔL can be negative; the plume would look cooler than the surrounding objects in the scene. If the plume and surface temperature are approximately equal then a ΔL near zero would be seen. An example of this would be the detection of plumes at distances away from the source where the plume has had time to mix with the

ambient air. Even extremely large concentrations of effluent might be undetectable if the temperature contrast were not present. The word "might" is used here to remind us that techniques which utilize other regions of the spectral band (outside of the LWIR) may be able to detect either an emissive temperature difference or possibly a reflected sunlight component of the plume. If the plume temperature is greater than the background temperature, then detection of the effluent is possible. In fact, both the effluent concentration and the temperature difference work to enhance the signal: as concentrations rise the plume transmission decreases and the second factor approaches one.

The question becomes which is the most important factor in modulating the cumulative radiance. Changes in the plume temperature are directly observed in the Planck emitted radiance, and similarly for the surface temperature. Modifying the effluent concentration results in an attenuation of the below plume radiance most significant in the effluent absorption band region, and in a change in the emissivity characteristics of the plume *($t_p \sim 1-\varepsilon_p$* in the LWIR). The increase in plume emission is partially balanced by a decrease in the surface emitted radiance passing through the plume and reaching the sensor. It can be seen that the effluent concentration modulates the radiance but the plume temperature determines both the baseline radiance and whether the plume scene radiance is less than the background radiance (as in the hot surface case) or greater than the background radiance (warm plume or cool surface). In the case where the plume, ambient and surface temperatures are identical, it would be very difficult to detect an effluent from the radiance signal alone.

An estimate of the effluent concentration can be obtained from the plume layer transmission t_p by solving (10) for t_p ,

$$t_p \cong 1 - \frac{\Delta L}{t_a \left\{ B\left[T_p\right] - \varepsilon_{sfc} B\left[T_{sfc}\right] \right\}} \quad . \tag{9}$$

The plume layer transmission $t_p = 10^{-\alpha}$ where α is the absorbance (related to the optical depth by a constant factor) of the plume. Therefore, the equation for α has the form,

$$\alpha = \log_{10} \left| x \right| - \log_{10} \left| x - \Delta L \right|, \quad where\ x = t_a \left\{ B\left[T_p\right] - \varepsilon_{sfc} B\left[T_{sfc}\right] \right\} \quad . \tag{10}$$

In (10) it is clear that the value of x must be greater than ΔL. As ΔL approaches zero (plume-free case), α goes to zero as expected and when $\Delta L = x\text{-}1$, the value for α is just $log_{10}|x|$. It is unlikely the latter value has any physical significance; its occurrence is most likely a factor of the assumptions made above. As ΔL approaches x, α becomes increasingly large. To improve the accuracy of the absorbance estimate, a small correction factor could be added to x to include the effects of the neglected reflected downwelling component in (7).

2.4 Detection Issues

The detection of an effluent plume from an airborne or spaceborne platform using an LWIR technique similar to the one described in the previous sections, requires accurate knowledge

of the intervening atmosphere (spectral transmission), the underlying surface (temperature and emissivity), and the spectral absorption characteristics of candidate gaseous species. Determination of the background radiation is the most important piece of information needed and probably the most difficult to estimate accurately. Errors can result from assuming the radiance from a nearby clear region is representative of the radiance underlying the plume. If a segment of the spectral band is known to be free of effluent absorption, then an estimate of the effective surface radiance $T_e = \varepsilon_s B[T_s]$ might be derived. However, knowledge of the variation in emissivity with wavelength is needed to accurately associate the derived value to other spectral bands. The separation of temperature and emissivity is a fundamental problem in the LWIR and several techniques have been published to address this issue[8,9,10,11].

The above approach assumes that the effluent species was known and the analyst knew where to look spectrally to find the telltale signal. Without this knowledge, a spectral matched filter technique or some other approach must be used to provide this information. Using a mathematical approach, gaseous absorption signatures from a spectral library are compared with the measured radiance (actually ΔL) to detect and identify the effluent species.

3. LWIR RADIATIVE TRANSFER MODEL

The technique used in this study to model the spectral radiance from a scene containing a plume layer consists of the following steps: 1) compute the layer optical depths using a line-by-line model such as FASE for atmospheric conditions approximating the plume-free scene conditions, 2) merge the spectral absorptivity of the selected effluents into the model plume layer, and 3) compute the atmospheric at-sensor radiance components using (3) and (5). The simulation of the scene radiance for plume cases was primarily used for the development of applications for FASSP[5]. It has proven a useful tool for the understanding of effects of plumes on the outgoing radiance field and provides a testbed for the ongoing effluent detection and identification study[12]. A brief description of the above steps follows.

3.1 Plume Scene Modeling Steps

Using atmospheric properties appropriate to the desired model parameters, FASE was run to produce optical depths at user-defined layers. Since only atmospheric parameters were calculated, no input surface information was needed. This approach allowed the definition of surface parameters at the time of the final radiance component calculation, without the need to rerun the line-by-line model. The full resolution layered optical depths were reduced to a resolution of 0.1 cm^{-1} using the procedure outlined in Griffin et al [6].

The characterization of the plume layer was done following the FASE calculations of the layered atmospheric optical depths. The effluent dispersion was derived from a gaussian plume model. This provided an estimate of the relative amount of effluent at a specified distance away from the source (in this case a stack of known height, diameter and outflow parameters). The effluent library contained the absorptivity as a function of wavelength and integrated gas amount (in PPM-m) for each effluent. Using the known effluent emission rate

(in g s^{-1}) and the estimated dispersed gas amount from the plume model, the corresponding spectral absorptivity of the gas to place into the plume layer was determined. In fact, multiple gases could be merged together using individual emission rates and spectral absorptivities to obtain a plume layer representative of a simultaneous release of many gases. For these cases, it was assumed that a single temperature was representative of all gases in the plume for a specific location away from the stack. Also, the spectral resolution of the effluent absorbances differed from the LWIR model spectral resolution. A cubic spline interpolation scheme was employed to convert the absorbances to a standard model resolution of 0.1 cm^{-1}.

A simple radiative transfer (RT) code was developed to utilize the computed layered transmittance information along with known atmospheric temperature profiles and modeled surface temperature and emissivities to compute the upwelling, downwelling, and surface emission components of the atmospheric radiative transfer. The assumption of a non-scattering (emission and absorption only) plane-parallel atmosphere was used to simplify the computations. These components can be computed for both the with-plume and without-plume atmospheric cases.

FASSP allows the user to simulate the at-sensor radiance for a variety of hyperspectral imagers including VNIR/SWIR sensors such as AVIRIS[13] and HYDICE[14] as well as MWIR/LWIR sensors such as SEBASS[15]. As a final step, the specific sensor response function was convolved with the modeled radiances to provide an estimate of the sensor-specific measured radiance for the plume scenario.

3.2 Modeling Examples

The LWIR RT code was used in conjunction with plume dispersion and sensor models to estimate the at-sensor radiance from a scene containing a gaseous plume. Figure 3a depicts the derived spectral radiances (shown as equivalent brightness temperatures, T_b) for a scene containing an active plume composed of a single gas (methanol) emitted from a stack at 20 m. The specific parameters for this scenario are given in Table 1. Some of the parameters are used in the plume concentration analysis (stack height, diameter, exit velocity, gas emission rate, wind speed, etc.) while others are used in the radiative transfer equations shown above (sensor altitude, surface and gas temperature) and in the sensor definition (sensor type and OPD). Included in Fig. 3a are the background T_b (dotted line in Fig. 3a) along with plots of the differential T_b (Fig. 3b), the plume emissivity (Fig. 3c) and the effluent absorbance (Fig 3d) as derived from (10). While the calculation of the absorbance is based upon radiance calculated from a scene containing prescribed gaseous amounts, it does still provide a consistency check on the methodology. For this case, the plume signature is easy to detect due to a combination of enhanced gas concentration and a warm plume temperature (approximately 20 K higher than the surrounding surface).

Table 1. Parameters used to estimate the at-sensor radiance from a scene containing a gas plume.

Parameter	Single Gas	Multiple Gases
Gas(es)	Methanol	Acetone, Methane, Sulfur Dioxide, Tetrachloroethylene
Gas Emission Rate(s) – g s^{-1}	10	7, 3, 25, 15
Gas Temperature (C)	40	20
Stack Height (m)	20	20
Stack Diameter (m)	0.3	0.3
Stack Exit Velocity (m s^{-1})	10	14
Atmospheric Model	Mid-latitude Summer	Sub-Arctic Summer
Wind Speed (m s^{-1})	5	10
Surface Temperature (C)	21.2	1.2
Sensor	Prism Spectrometer	FTS
Sensor Altitude (km)	2.8	3.5
Sensor OPD (cm)	-	0.25

A second scenario consisted of a plume containing four gases each with a unique emission rate as shown in Table 1. For this case the at-sensor radiance from the plume and background was modeled for a notional Fourier Transform Spectrometer (FTS) with an Optical Path Difference (OPD) of 0.25 cm. This corresponds to a spectral resolution of approximately 2 cm^{-1}. The graphs in Fig. 4 corresponding to the derived T_bs, plume emissivity and absorbance are analogous to those presented in Fig. 3. However, in this case, overlap of the effluent signatures makes it more difficult to identify individual contributions. Fig. 4d displays the total plume absorbance overlaid on top of the individual absorbances for the four gases used in the simulation. The displayed integrated concentrations (in PPM-m) were found by manually adjusting the standard gas concentrations so that specific gas absorbance features were in agreement with the total plume absorbance. Automation of this step is under development using a spectrally matched filter technique.

4. SUMMARY

Measurements of outgoing radiance in the LWIR are known to be useful for detection and quantification of gaseous absorbers. A model originally developed to provide hyperspectral sensor system analyses has been modified to allow simulation and analysis in the LWIR of scenes containing gaseous effluents emitted from a known source. This model provides a testbed to simulate the at-sensor radiance measurements from current and future sensors for cases of plumes containing one or more gaseous absorbers each with unique emission rates. The model computes the integrated effluent concentrations and merges that information with atmospheric optical depths computed from a line-by-line radiative transfer model. A component radiative transfer model allows estimation of the radiance components of the plume, surface, atmosphere and the total at-sensor amount.

Equations describing the individual radiance components were presented for transfer through the plume and for a clear atmosphere. The differential radiance was computed and a simplified form was derived which allowed estimation of the contributions from the three major components to be compared: the atmospheric transmittance, the plume emissivity, and the plume/surface radiance difference. While the transmittance and plume emissivity contributed to the magnitude of the plume signal, the plume/surface temperature difference contributed not only to the magnitude but determined whether an emission (positive differential radiance) or absorption (negative differential radiance) effect was dominant.

Examples were shown for cases with single and multiple gas plumes. For single gases of sufficient concentration and temperature difference, it is generally easy to separate the plume signature from the background radiance. For plume cases with multiple gas components, overlap of the gaseous absorbance can mask individual signatures making identification of

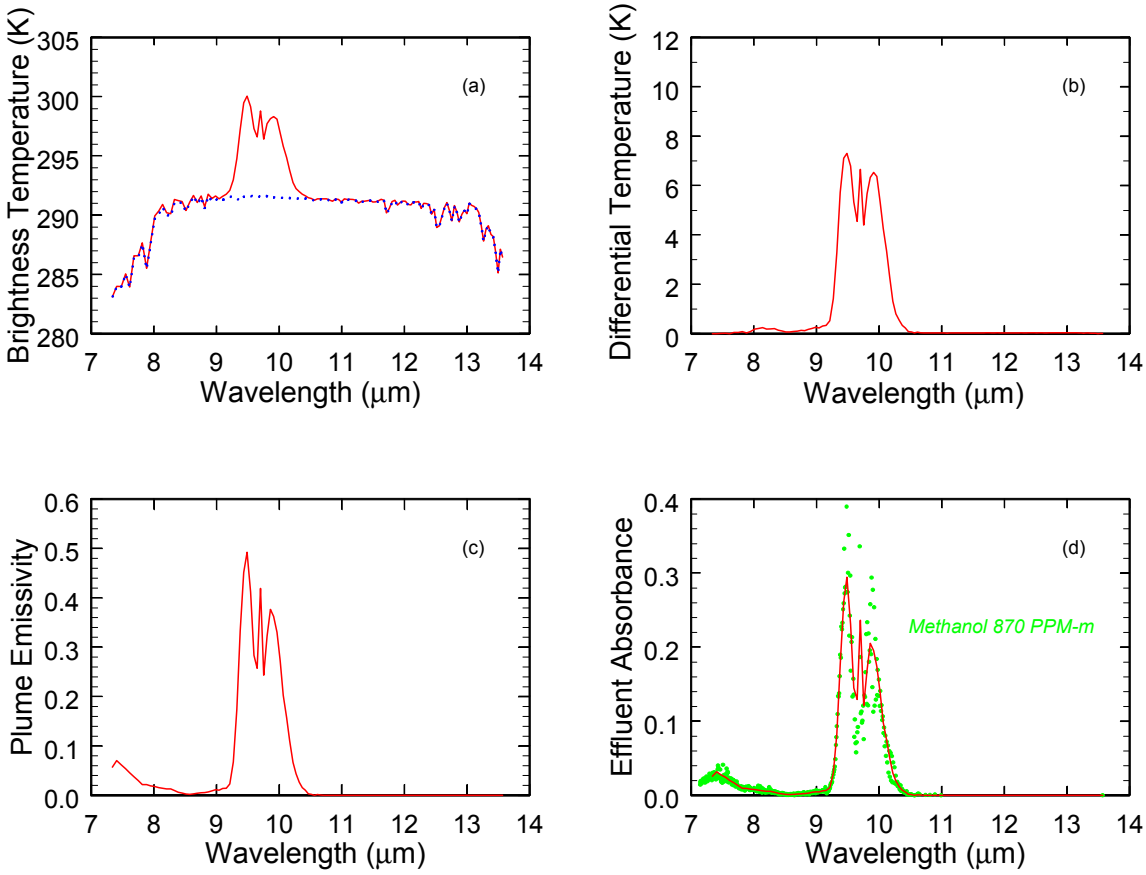

Figure 3. Plots of various components as a function of wavelength for a scene containing a gaseous effluent (Methanol). The four plots show a) the brightness temperature for both the plume (solid) and background (dotted), b) the differential brightness temperature, c) the plume emissivity and d) the derived (solid) and input "true" (dotted) effluent absorbance.

gases difficult. A good example of this would be volcanic emissions which quite often contain not only sulfur dioxide (a primary constituent of volcanic gas), but enhanced amounts of water vapor, carbon dioxide, hydrogen sulfide and other gases which are generally emitted at temperatures much higher than the ambient. The broad extent of water vapor absorption in the LWIR can make estimation of the amount of the other constituents a complex undertaking. While a manual technique was used here to extract the individual gas signatures from the total plume absorbance, other techniques such as spectral matched filter might provide a way to automate the process.

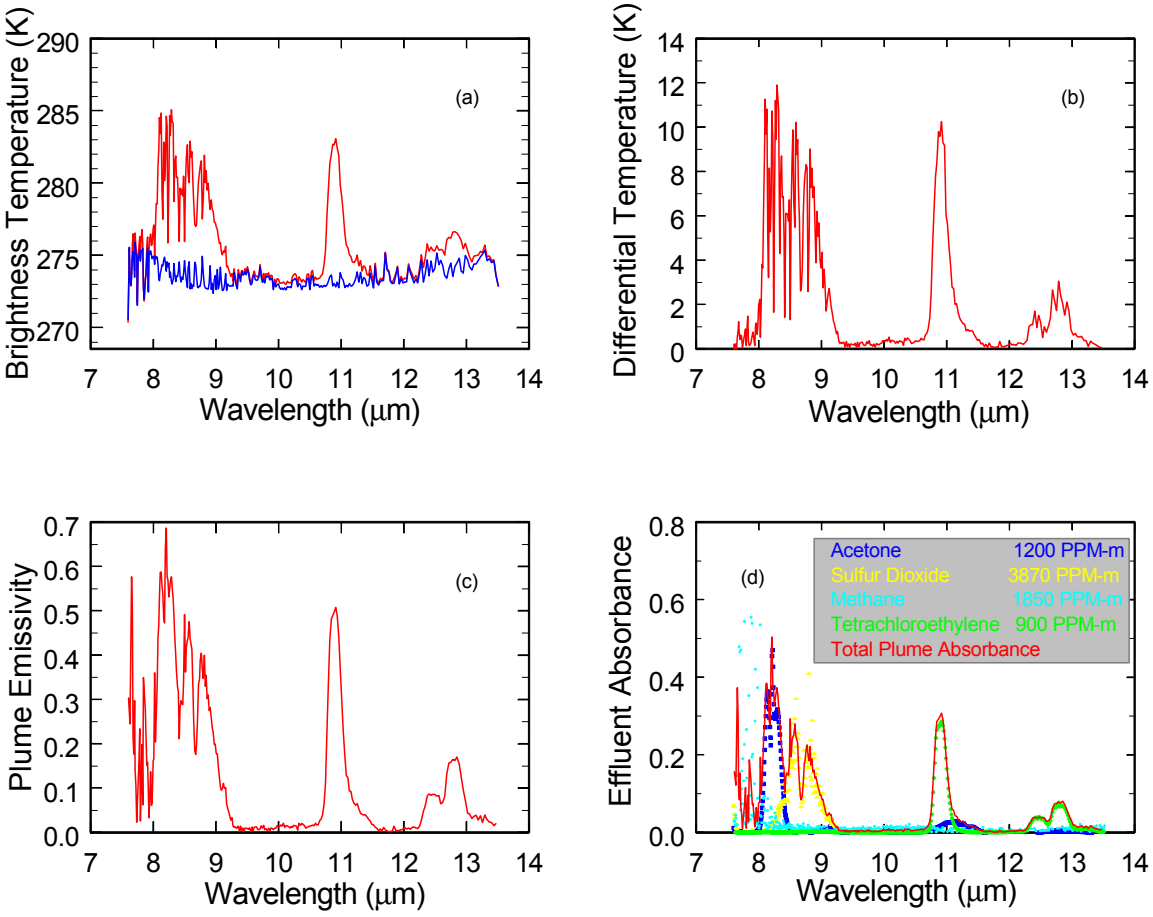

Figure 4. Similar to Fig. 3 except the scenario includes four gases: acetone, sulfur dioxide, methane and tetrachloroethylene.

REFERENCES

1. Berk, A, L.S. Bernstein, G.P. Anderson, P.K. Acharya, D.C. Robertson, J.H. Chetwynd, and S.M. Adler-Golden, 1998: "MODTRAN Cloud and Multiple Scattering Upgrades with Application to AVIRIS." *Remote Sens. Environ*., **65**, 367-375.
2. Snell, H.E., G.P. Anderson, J. Wang, J.-L. Moncet, J.H. Chetwynd, and S.J. English, 1995: "Validation of FASE (FASCODE for the Environment) and MODTRAN3: Updates and Comparisons with Clear-Sky Measurements." *Proceedings of Passive Infrared Remote Sensing of Clouds and the Atmosphere III*, SPIE **2578**, Orlando, FL, 194-204.
3. Smith, H.J.P., D.J. Dube, M.E. Gardner, S.A. Clough, F.X. Kneizys and L.S. Rothman, 1978: "FASCODE – Fast Atmospheric Signature CODE (Spectral Transmittance and Radiance)." *Air Force Geophysics laboratory, AFGL-TR-78-0081,* 149 pp.
4. Smith, B.W., editor, C.C. Borel, W.B. Clodius, A.B. Davis, P. Smolarkiewicz, J.J. Szymanski, J. Theiler, P.V. Villeneuve, A. Garrett and L. O'Steen, 1998: "Handbook of Science Algorithms for the Multispectral Thermal Imager." *Los Alamos National Laboratory, LA-UR-98-306,* 130 pp.
5. Kerekes, J.P., J.E. Baum and K.E. Farrar, 1999: "Analytical Model of Hyperspectral System Performance." *SPIE Aerosense 1999,* **3701**, Orlando, FL, pp 155-166.
6. Griffin, M.K., H.K. Burke, C.M. Richard, and J.P. Kerekes, 2000: "Characterization of Gaseous Effluents in the LWIR." *Proceedings of the Multi/Hyperspectral Sensors, Measurements, Modeling and Simulation Workshop*, Huntsville, AL.
7. Rothman, L.S., C.P. Rinsland, A. Goldman, S.T. Massie, D.P. Edwards, J.-M. Flaud, A. Perrin, C. Camy-Peyret, V. Dana, J.-Y. Mandin, J. Schroeder, A. McCann, R.R. Gamache, R.B. Wattson, K. Yoshino, K.V. Chance, K.W. Jucks, L.R. Brown, V. Nemtchinov and P. Varanasi, 1998: "The HITRAN Molecular Spectroscopic Database and HAWKS (HITRAN Atmospheric Workstation): 1996 Edition." *J. Quan. Spectr. and Rad. Trans.*, **60**, pp. 665-710.
8. Matsumoto-Moriyama, M. and K. Arai, 1994: "An Inversion for Emissivity-Temperature Separation with ASTER Data." *Adv. Space Res.,* **14**, No. 3, pp. 67-70.
9. Borel, C.C., 1997: "Iterative Retrieval of Surface Emissivity and Temperature for a Hyperspectral Sensor." *First JPL Workshop on Remote Sensing of Land Surface Emissivity,* Pasadena, CA, pp. 1-5.
10. Gillespie, A.R., S. Rokugawa, S.J. Hook, T. Matsunaga and A.B. Kahle, 1999: "Temperature/emissivity Separation Algorithm Theoretical Basis document, Version 2.3." ATBD contract NAS5-31372, NASA.
11. Li, Z-L, F. Becker, M.P. Stoll and Z. Wan, 1999: "Evaluation of Different methods for Extracting Relative Spectral Emissivity Information from Simulated Thermal Infrared Multispectral Scanner Data." *Rem. Sens. Environ*., **69**, pp. 122-138.

12. Kerekes, J.P., M.K. Griffin, J.E. Baum and K.E. Farrar, 2001: Modeling of LWIR Hyperspectral System Performance for Surface Object and Effluent Detection Applications." *SPIE Aerosense,* **4381**, Orlando, FL.

13. Vane, G., R.O. Green, T.G. Chrien, H.T. Enmark, E.G. Hansen, and W.M. Porter, "The Airborne Visible/Infrared Imaging Spectrometer (AVIRIS)," *Remote Sensing Environ.*, **44**, pp. 127-143, 1993.

14. Rickard, L.J., R. Basedow, E. Zalewski, P. Silverglate, and L.M. Lander, "HYDICE: An Airborne System for Hyperspectral Imaging," *SPIE 1993 Proceedings,* **1937**, pp. 173-179, Orlando FL, 1993.

15. Hackwell, J.A, et al., 1996: "LWIR/MWIR Imaging Hyperspectral Sensor for Airborne and Ground-Based Remote Sensing." *SPIE Aerosense 1996*, **2519**, Orlando, FL, pp 102-107.

ACKNOWLEDGEMENTS

The authors wish to thank CAPT Frank Garcia at DUSD (S&T), program manager for the Hyperspectral Technology Assessment Program (HTAP) at Lincoln Laboratory for his support of this effort.